ACS OMEGA

Open Access

http://pubs.acs.org/journal/acsodf

Article

Quencher-Free Fluorescence Monitoring of G-Quadruplex Folding

Zachary Parada, Tanner G. Hoog, Katarzyna P. Adamala, and Aaron E. Engelhart*

Cite This: *ACS Omega* 2025, 10, 3176−3181

Read Online

ACCESS | Metrics & More | Article Recommendations | Supporting Information

ABSTRACT: Guanine-rich sequences exhibit a high degree of polymorphism and can form single-stranded, Watson−Crick duplex, and four-stranded G-quadruplex structures. These sequences have found a wide range of uses in synthetic biology applications, arising in part from their structural plasticity. High-throughput, low-cost tools for monitoring the folding and unfolding transitions of G-rich sequences would provide an enabling technology for accelerating the prototyping of synthetic biological systems and for accelerating design−build−test cycles. Here, we show that unfolding transitions of a range of G-quadruplex-forming DNA sequences can be monitored in a FRET-like format using DNA sequences that possess only a single dye label, with no quencher. These quencher-free assays can be performed at low cost, with both cost and lead times ca. 1 order of magnitude lower than FRET-labeled strands. Thus, quencher-free secondary structure monitoring promises to be a valuable tool for the testing and development of synthetic biology systems employing G-quadruplexes.

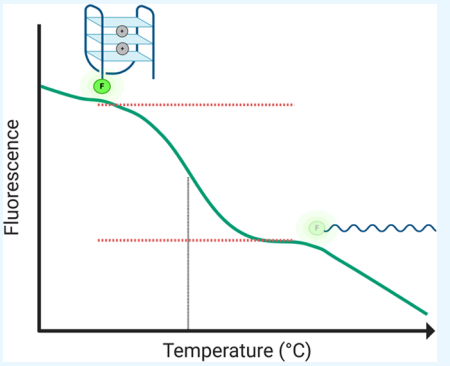

INTRODUCTION

Guanine-rich sequences exhibit an unusual degree of polymorphism among nucleic acids.[1,2] In addition to their single-stranded and Watson−Crick duplex forms, G-rich sequences can exist in equilibria with four-stranded structures called G-quadruplexes, which form via Watson−Crick−Hoogsteen interactions between quartets of four guanines, which in turn coordinate a central cation. G-quadruplex (G4) structures have been employed in a range of synthetic biology applications, including sensing of diverse ligands for readout of metabolic states,[3−6] forming nucleic acid−based nanomachines,[7,8] and biomimetic cofactor binding that enables catalysis of a wide range of electron transfer reactions.[9−12] Monitoring the polymorphism and folding states of G-rich sequences is key to understanding their function. A variety of techniques have been employed for such monitoring, including high-resolution structural techniques such as NMR and crystallography,[13−16] as well as higher-throughput spectroscopic techniques, including circular dichroism and FRET.[17,18] Of these, FRET is among the most widely used, due to its experimental expediency and high throughput.[19]

In a typical execution, FRET experiments employ a fluorophore as a donor, and a second dye as an acceptor—typically one with low fluorescence quantum yield, which acts as a quencher. These experiments require the synthesis of dual-labeled probes. These probes have high associated cost, greater lead time, and low yields arising from the need to incorporate both 3′ and 5′ modifications and perform HPLC purification. While quencher-free systems have been employed for monitoring hybridization in molecular beacons and similar probes, these applications typically employ bespoke dyes in hairpin structures.[20−22] Our study focuses on the application of quencher-free fluorescence monitoring with a standard dye (fluorescein) for G-quadruplex (G4) identification.

While performing FRET characterization of a switchable G4-based nucleic acid electron transfer catalyst,[11] we serendipitously observed that a singly labeled G-rich oligonucleotide provided FRET-like curves that acted as a reporter of strand folding state, with the G4 state of a singly labeled strand giving high fluorescence, and the single-stranded (ss) state giving low fluorescence. The crux of our study lies in the understanding that, within a G-quadruplex structure, guanine bases are closely associated, participating in a network of $\pi-\pi$ interactions that stabilize the quadruplex formation. Upon the unfolding of these structures, the spatial arrangement of guanine bases is disrupted, leading to an increase in the accessibility of these bases. This effect is anticipated to be more pronounced in the context of our ssDNA constructs, where the adjacent guanine runs, once part of a stable G-quadruplex, are now exposed. These guanine runs upon G-quadruplex unfolding exhibit a noticeable decrease in fluorescence, serving as a direct monitor of the structural transition.

The adoption of singly modified dye-labeled oligonucleotides promises significant simplification and cost reduction in experimental workflows. These variants are more readily synthesized compared to dual-labeled oligonucleotides. For instance, a 26-nt 5′-fluorescein-labeled oligonucleotide at the

Received: November 25, 2024
Revised: December 12, 2024
Accepted: December 19, 2024
Published: January 15, 2025

same scale costs 12% as much (2024 prices) as the same 26-nt 5′-fluorescein-labeled, 3′-Iowa Black-labeled oligonucleotide. Additionally, the singly labeled oligonucleotide has a lead time of 2 business days while the dual-labeled oligonucleotide has a lead time of 9 business days. This reduction in both cost and lead time would greatly facilitate rapid prototyping and design−build−test cycles. Encouraged by this prospect, we investigated whether the secondary structure-dependent fluorescence observed in singly labeled oligonucleotides is a widespread phenomenon.

RESULTS AND DISCUSSION

We characterized a range of oligonucleotides (Table 1) capable of forming G4 structures by both fluorescence and UV absorbance (Figure 1). As a benchmark, we initially examined the fluorescence and UV absorbance thermal transitions of **FAM-G4-IB**, a G4-forming oligonucleotide with a 5′-fluorescein and 3′-Iowa Black quencher (Figure 1a−b, Table 1). As expected, **FAM-G4-IB** gave a cooperative transition, indicative of a G-quadruplex (G4) to single-strand (ss) transition. In the absorbance trace, a decrease in absorbance at 295 nm was observed, consistent with the unfolding of a G4. In the fluorescence trace, the G4 state gave low fluorescence, and the ss state gave high fluorescence, consistent with the closer positioning of the 5′ dye label and 3′ quencher in space in the folded G4 state relative to the unfolded ss state. Both fluorescence and absorbance traces gave T_M values that agreed with one another, consistent with both spectroscopic techniques reporting on the same unfolding transition in potassium buffer (Figure 1b, Supporting Information Tables 1 and 2), as well as sodium buffer (Supporting Information Figure 1a).

Table 1. List of Oligonucleotides Used in This Work

sequence name	description	sequence (5′−3′)
FAM-G4-IB	FAM-G4 Sequence-Iowa Black	/56-FAM/TGG GTT AGG GAA TTC GGG TTA GGG/3IABkFQ/
FAM-G4	FAM-G4 Sequence	/56-FAM/TGG GTT AGG GAA TTC GGG TTA GGG
HT	FAM-Human Telomere	/56-FAM/GGG TTA GGG TTA GGG TTA GGG
HT-T	FAM-Human Telomere - T spacer	/56-FAM/TGG GTT AGG GTT AGG GTT AGG G
HT-C	FAM-Human Telomere - C spacer	/56-FAM/CGG GTT AGG GTT AGG GTT AGG G
HT-A	FAM-Human Telomere - A spacer	/56-FAM/AGG GTT AGG GTT AGG GTT AGG G
HT-TT	FAM-Human Telomere - TT spacer	/56-FAM/TTG GGT TAG GGT TAG GGT TAG GG
HT-TTA	FAM-Human Telomere - TTA spacer	/56-FAM/TTA GGG TTA GGG TTA GGG TTA GGG
EHT	FAM-Expanded Human Telomere	/56-FAM/TGG GGT TAG GGG TTA GGG GTT AGG GG
TBA	FAM-Thrombin Binding Aptamer	/56-FAM/GGT TGG TGT GGT TGG
TBA-T	FAM-Thrombin Binding Aptamer - T spacer	/56-FAM/TGG TTG GTG TGG TTG G
TBA-C	FAM-Thrombin Binding Aptamer - C spacer	/56-FAM/CGG TTG GTG TGG TTG G
TBA-A	FAM-Thrombin Binding Aptamer - A spacer	/56-FAM/AGG TTG GTG TGG TTG G
TBA-TT	FAM-Thrombin Binding Aptamer - TT spacer	/56-FAM/TTG GTT GGT GTG GTT GG
TBA-TTA	FAM-Thrombin Binding Aptamer - TTA spacer	/56-FAM/TTA GGT TGG TGT GGT TGG
ETBA	FAM - Expanded Thrombin Binding Aptamer	/56-FAM/TGG GTT GGG TGT GGG TTG GG
non-G4	FAM-Duplex Top Strand	/56-FAM/CGA CTA TGA GGA TCT C
HT-2	Human Telomere 2	/56-FAM/TG GGT TAG GGT TAG GGT TAG GGT T
HT-2-I	Human Telomere 2 Isomer	/56-FAM/TG TGT GAG TGT GAG TGT GAG TGT G

We next examined **FAM-G4**, the same sequence as **FAM-G4-IB**, with only a 5′-fluorescein end label and no 3′-quencher. This sequence also gave a quencher-free-fluorescence melting profile that corresponded with that observed by absorbance spectroscopy (K^+: Figure 1c, Na^+: Supporting Information Figure 1b). The fluorescence trace for **FAM-G4** trace was the inverse of that observed for **FAM-G4-IB**, with **FAM-G4** giving high fluorescence in the G4 state and low fluorescence in the ss state. The unfolding transition of **FAM-G4-IB** was stabilized relative to **FAM-G4** (56.9 °C vs 38.6 °C in potassium solution, Supporting Information Table 2) consistent with previous reports of stabilizing interactions associated with oligonucleotide labels.[23]

We examined a suite of other G4-forming oligonucleotides. The G4 formed by four copies of the human telomere sequence d(TTAGGG) (**HT**, K^+: Figure 1d, Na^+: Supporting Information Figure 1c)[24] exhibited the same behavior, with good agreement between absorbance and quencher-free-fluorescence traces. An expanded variant of this sequence with repeats of d(TTAGGGG) (**EHT**, K^+: Figure 1e, Na^+: Supporting Information Figure 1d) also showed similar behavior.

We next sought to examine an aptamer sequence, as G-quadruplex structures are often found in this important class of functional RNA.[25] The thrombin binding aptamer (**TBA**, K^+: Figure 1f, Na^+: Supporting Information Figure 1e),[26] which contains a G4 with only two guanine quartets, is known to fold stably in potassium, but not sodium solution. As expected, quencher-free-fluorescence and absorbance spectra reflected the presence of a cooperative unfolding transition in potassium, but not sodium solution. An expanded version of this aptamer with a three-guanine quartet core (**ETBA**, K^+: Figure 1g, Na^+: Supporting Information Figure 1f) gave the expected increased stabilization relative to **TBA** and concurrence between quencher-free-fluorescence and absorbance traces as well. We observed agreement between quencher-free-fluorescence and absorbance traces for all G4-forming sequences tested (Supporting Information Tables 1 and 2).

Guanine possesses the lowest redox potential of the canonical nucleobases,[27,28] and due to this, it is well-known to nonspecifically quench fluorescence by a mechanism that is thought to involve photoinduced electron transfer. Because of this, it is typically not recommended to have a guanine residue immediately adjacent to a dye label. The sequence we initially tested possessed no spacer between the dye and G4-forming sequence (K^+: **HT**, Figure 2a/**TBA**, Figure 2b, Na^+: **HT**, Supporting Information Figure 2a/TBA, Supporting Information Figure 2b). As expected, this gave the lowest fluorescence of the sequences tested, with fluorescence suppressed by 30−50% relative to labeled oligonucleotides with no spacer residue. Despite this, it still could report on unfolding, consistent with the formation of a G4 structure relieving guanosine-induced fluorescence quenching. Multiple possibilities exist to explain

https://doi.org/10.1021/acsomega.4c10720
ACS Omega 2025, 10, 3176−3181

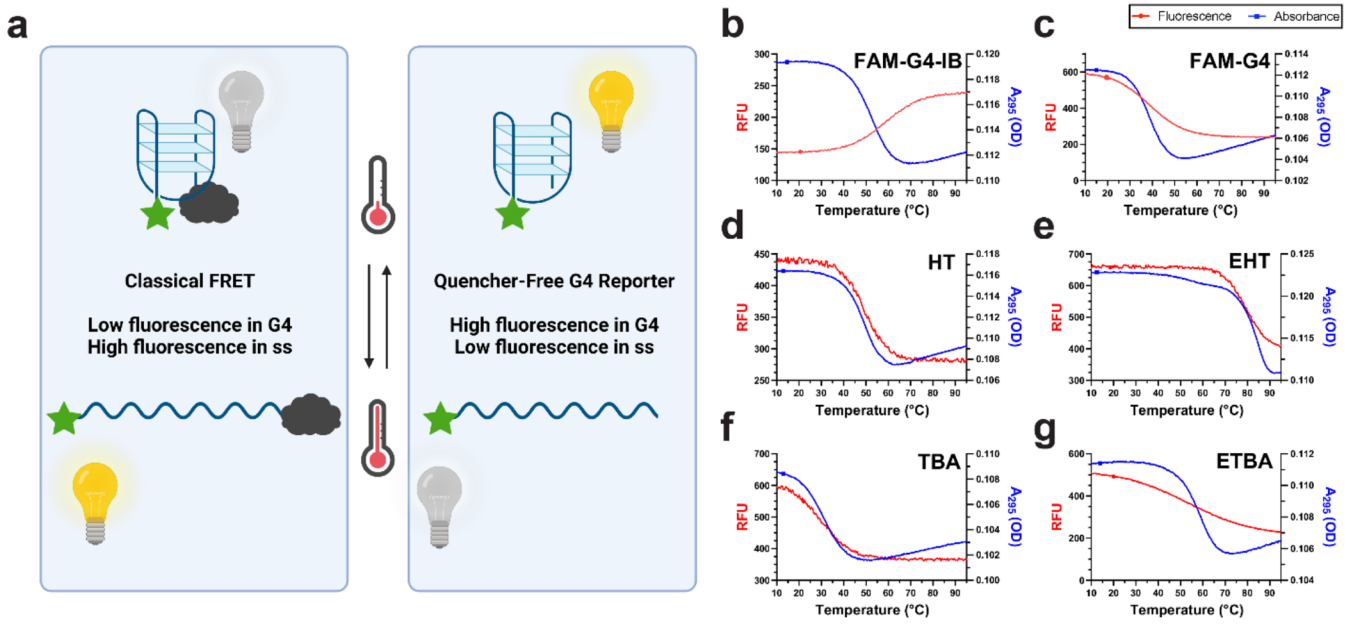

Figure 1. Quencher-free fluorescence- and absorbance-monitored thermal denaturation profiles both report on unfolding of various G-Quadruplex-forming sequences. (a) Graphical comparison of classical FRET and quencher-free fluorescence monitoring of unfolding transitions, (b) FAM-G4-IB with fluorescein and Iowa Black quencher, (c) FAM-G4 with only fluorescein modification, (d) HT with four repeats of human telomere sequence, (e) EHT, a variant of HT with an expanded G-tract. (f) TBA, the 15 nt thrombin binding aptamer, (g) ETBA, a variant of TBA with an expanded G-tract. Cooperative transitions were observed in all cases, indicating G-quadruplex to single-stranded transitions. All data shown were collected in K^+-containing buffer.

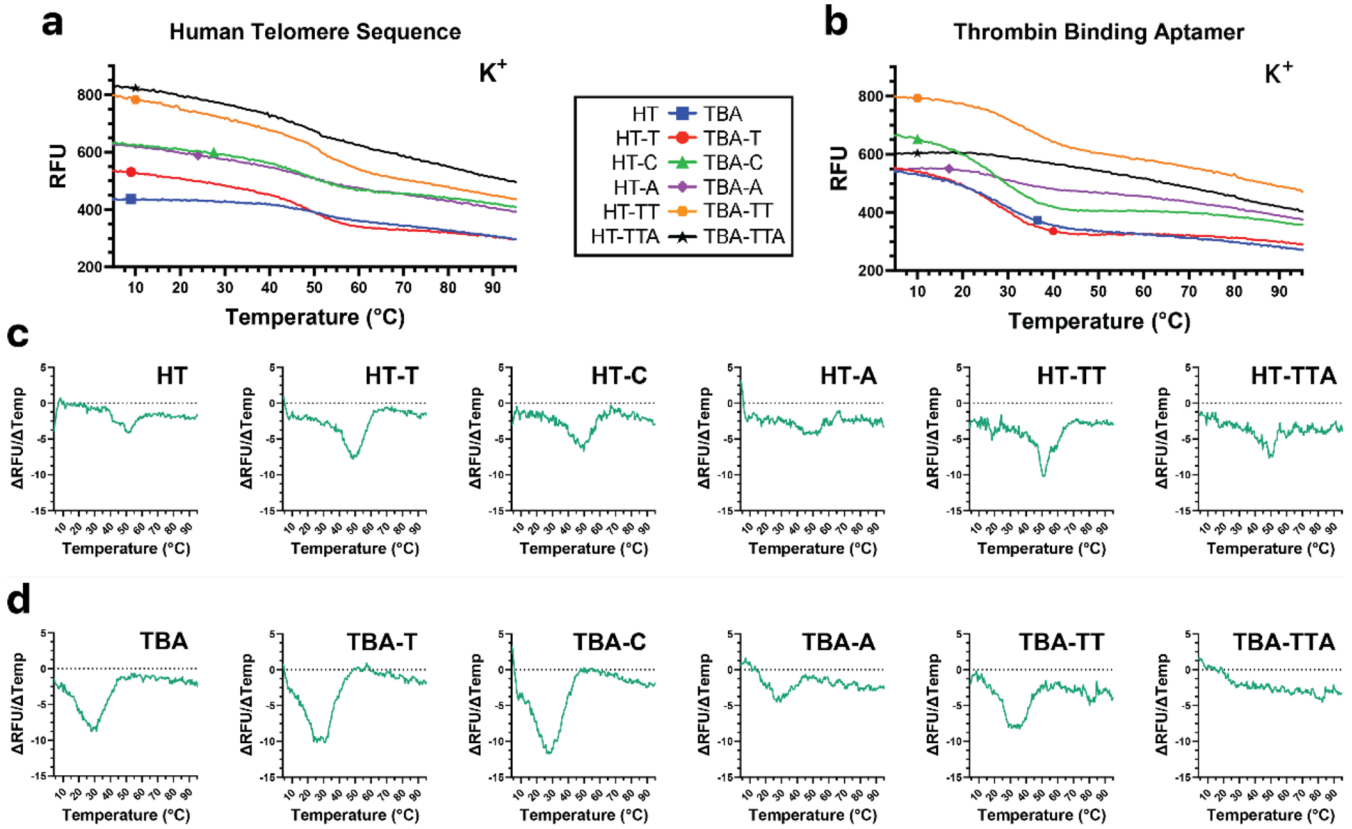

Figure 2. Influence of fluorophore proximity and spacer sequences on fluorescence transitions in various oligonucleotide G-tracts. (a) Fluorescence thermal melts of human telomere sequence (HT) with zero-, single-, or multiple-nucleotide spacers. (b) Fluorescence thermal melts of thrombin binding aptamer (TBA) with zero-, single- or multiple-nucleotide spacers. (c) First derivatives of HT fluorescence vs temperature with single or multiple-nucleotide spacers (d) First derivatives of TBA fluorescence vs temperature values with single or multiple-nucleotide spacers. All data shown were collected in K+-containing buffer.

https://doi.org/10.1021/acsomega.4c10720
ACS Omega 2025, 10, 3176−3181

differential quenching phenomena in labeled strands. Electronic effects of adjacent bases, number of guanines (i.e., runs of 2 vs 3 guanines), and three-dimensional folding state of oligonucleotides are three possibilities.

We sought to investigate whether the secondary structure-dependent effect we observed was dependent on the presence of "spacer" nucleotide residues between the 5′-dye label and the sequence being interrogated for folding activity. Accordingly, we prepared analogues of the **HT** and **TBA** sequences with variable spacers between the 5′-fluorescent residue and the G4-forming sequence of interest (Figure 2). We examined sequences containing a spacer consisting of each nonguanosine nucleotide: thymine (**HT-T**/**TBA-T**), cytosine (**HT-C**/**TBA-C**), and adenine (**HT-A**/**TBA-A**). Each of these sequences gave higher fluorescence values than the spacer-free sequences **HT** and **TBA**, with similar capacity to report on unfolding transitions (K^+: Figure 2, Na^+ Supporting Information Figure 2).

Finally, we examined sequences containing longer dinucleotide (d(TT), **HT-TT**/**TBA-TT**) or trinucleotide (d(TTA), **HT-TTA**/**TBA-TTA**) spacers. Here, **TBA-TT** and **HT-TT** gave better performance as reporters than **TBA-TTA** or **HT-TTA**. In the case of d(TTA)-spacer containing oligonucleotides, only the potassium form of **TBA-TTA** gave a clear transition by fluorescence (K^+: Figure 2, Na^+ Supporting Information Figure 2).

Multiple possibilities exist to explain differential quenching phenomena in labeled strands, including electronic effects of adjacent bases, variations in the number of guanines (i.e., runs of two vs three guanines), and the three-dimensional folding state of the oligonucleotides. To investigate the impact of folding state, we examined **TBA** and **HT** by circular dichroism. Consistent with our other results and prior reports on the unlabeled strand, only the potassium form of **TBA** was folded into a G-quadruplex (Supporting Information Figure 3). **HT** gave cation-dependent topologies, with the sodium form exhibiting spectra consistent with an antiparallel topology and the potassium form exhibiting a hybrid topology (Supporting Information Figure 4). Thus, the different three-dimensional orientation of the sodium and potassium forms of **HT** could explain, in part, the differential quenching phenomena observed in **HT-TTA**, which approaches the limit of spacer length for quencher-free fluorescence monitoring of G4 folding. These findings illustrate that considerable sequence flexibility exists, as evidenced by strands containing A, T, and C spacers, but the TTA spacer results are consistent with an exquisitely distance-dependent short-range quenching phenomenon that is best employed for reporting on local folding and unfolding transitions. Circular dichroism of the spacer variants for both **TBA** and **HT**-derived sequences gave spectra consistent with no major global folding or topological changes across spacer variants (Supporting Information Figures 3 and 4g–h). Both these results and the consistency between fluorescence and absorbance melting temperatures (Supporting Information Tables 1 and 2) are consistent with the observed fluorescence changes arising from the folded-to-unfolded transition and not changes in topology.

To further verify that the observed fluorescence transitions resulted specifically from G4 formation and denaturation, we compared another G-quadruplex-forming human telomere sequence **HT-2** with its isomer **HT-2-I**, which was scrambled to disrupt G-tracts and suppress G-quadruplex formation (Supporting Information Figure 5). **HT-2** was selected because it contained an equal number of G and non-G residues, enabling generation of the scrambled sequence **HT-2-I** with no consecutive guanine residues. We used **HT-2** Quencher-free fluorescence and absorbance monitoring of thermal melts of **HT-2** showed unfolding of G-quadruplexes, as expected. Despite identical guanine content in the two sequences, **HT-2-I** did not exhibit transitions in quencher-free fluorescence or UV–vis absorbance thermal melts of **HT-2**, consistent with the requirement for G-tracts for quenching in the single-stranded state, and for folding into a G-quadruplex structure to relieve this quenching.

Guanosine-mediated fluorescence quenching has been employed to monitor a range of phenomena, including hybridization, DNA processing, ribozyme kinetics, and nucleotide cleavage.[29−35] The results presented here extend the utility of this quenching phenomenon to a monitoring of the folding state of a G-quadruplex-forming strand. As G-quadruplex secondary structures continue to find increasing utility in a wide range of synthetic biology applications, we anticipate that the low-cost, high-throughput detection method afforded by quencher-free fluorescence monitoring of these unfolding transitions will provide an enabling technology for accelerating design–build–test cycles in these and other applications. In another study of FRET-labeled G-quadruplexes, a fluorescein-labeled oligonucleotide showed different structure-dependent quenching behavior.[36] This work employed a different buffer and an unspecified linkage that may have varied from ours, based on the age of the manuscript and a fluorescein labeling method cited in the work.[37] While our results are consistent among a range of sequence and linker contexts, these results indicate that the structure-dependent fluorescence behavior of specific dyes or labeling methods may vary.

Our results also extend the literature on guanine-mediated single electron transfer reactions. The propensity of guanosine for oxidation has been invoked to explain the excited-state quenching observed when guanine nucleobases are present immediately adjacent to a fluorophore, as well as the sequence specificity associated with DNA damage and conductive behavior within DNA.[38] Our results illustrate that guanine-associated quenching is influenced by nucleic acid secondary structure. Thus, other single-electron transfer reactions in which guanine acts as an electron donor could be similarly influenced by secondary structure.

MATERIALS AND METHODS

Buffers. All experimental data were obtained using a 50 mM Li-HEPES buffer at pH 7.4. Each buffer additionally contained an alkali chloride salt. The lithium-containing buffer contained 50 mM LiCl (Sigma 203637), sodium-containing buffer contained 50 mM NaCl (VWR MK754006), and potassium-containing buffer contained 20 mM KCl (Sigma P9333).

DNA Sample Preparation. All DNA oligonucleotides were procured from Integrated DNA Technologies as desalted grade (unlabeled or singly labeled) or HPLC purified (dual-labeled). Oligonucleotides were resuspended in water to prepare 100 μM stocks. Individual oligonucleotide stocks were further quantified through UV absorption at 260 nm and diluted to 50 μM substocks for subsequent use; these stocks were stored at −20 °C. Upon dilution into the appropriate buffer and prior to use, all samples underwent prefolding by heating to 95 °C for 5 min, followed by cooling to room

https://doi.org/10.1021/acsomega.4c10720
ACS Omega 2025, 10, 3176−3181

temperature over a 3-h period. Fluorescence melts contained 200 nM 5′-fluorescein-labeled oligonucleotide, UV absorbance melts contained 5 μM 5′-fluorescein-labeled oligonucleotide, while circular dichroism samples contained 20 μM 5′ fluorescein-labeled oligonucleotide. Sequences for oligonucleotides employed are given in Table 1.

Fluorescence-Monitored Thermal Melts. Fluorescence measurements were performed using a Cary Eclipse fluorescence spectrophotometer (Agilent Technologies) equipped with a Peltier thermostated multicell holder (Agilent Technologies). The excitation wavelength was set to 495 nm, and the emission wavelength was set to 520 nm. Excitation slits were set to 2.5 nm and emission slits were set to 5 nm. The photomultiplier tube (PMT) voltage was set to 565 V. After prefolding (see DNA Sample Preparation), all samples underwent a temperature ramp from 4 to 100 °C at a rate of 0.5 °C/min to minimize hysteresis. This was followed by a 1 min hold at 100 °C, a subsequent cooling phase from 100 to 4 °C at the same rate, and an additional 1 min hold period at 4 °C. Fluorescence measurements were taken at 0.5 °C intervals, with a signal averaging time of 0.25 s. Two heat/cool cycles were performed by repeating this experimental sequence twice.

UV−vis-Monitored Thermal Melts. Thermal denaturation experiments were performed using a Cary 60 UV−vis spectrophotometer (Agilent Technologies), equipped with a qCHANGER 6 temperature-controlled linear cuvette changer (Quantum Northwest) controlled by a TC 1/Multi temperature controller (Quantum Northwest). Liquid cooling for the Peltier device was provided by a EX2-755 liquid cooling system (Koolance). The above instruments were interfaced using Cary ADL scripts (Quantum Northwest) that allowed monitoring of absorbance vs temperature at 295 nm. This allowed monitoring of G-quadruplex folding transitions. After prefolding (see DNA Sample Preparation), samples were heated from 10 to 100 °C and then cooled from 100 to 10 °C, using 0.5 °C steps for each ramp. At each step, a 30-s hold was performed before each reading with a signal averaging time of 0.25 s. This protocol gave approximately the same ramp times as that for the fluorescence experiments described above.

Circular Dichroism Spectroscopy for G-Quadruplex Topologies. Circular Dichroism (CD) measurements were carried out using a J-815 spectropolarimeter (Jasco) equipped with a Peltier temperature controller (Jasco). CD spectra were recorded between 220 and 320 nm, with continuous scanning mode and a scanning speed of 100 nm/min. The data integration time was fixed at 4 s per data point, and a data pitch of 1 and 2 nm bandwidth.

Data Analysis. Data from fluorescence and absorbance melting experiments were imported using MATLAB 2023a software (MathWorks). Subsequently, individual traces were plotted, and thermal midpoints were identified utilizing Igor Pro version 9 software (WaveMetrics). These midpoints were determined as the inflection points of sigmoidal fits corresponding to each respective heating or cooling transition. The recorded thermal midpoints are provided in Supporting Information Tables 1 and 2. Circular dichroism data was imported directly into GraphPad Prism v. 10.1.1 for processing and graphical representation.

■ ASSOCIATED CONTENT

Data Availability Statement

The data used are available throughout the manuscript text and in the Supporting Information.

Supporting Information

The Supporting Information is available free of charge at https://pubs.acs.org/doi/10.1021/acsomega.4c10720.

Fluorescence and UV absorbance thermal melting data, circular dichroism spectra for G-quadruplex characterization, and control experiments with an isomeric sequence not predicted to form a G-quadruplex (PDF)

■ AUTHOR INFORMATION

Corresponding Author

Aaron E. Engelhart − *Department of Biochemistry, Molecular Biology and Biophysics, University of Minnesota, Minneapolis, Minnesota 55455, United States; Department of Genetics, Cell Biology, and Development, University of Minnesota, Minneapolis, Minnesota 55455, United States;* orcid.org/0000-0002-1849-7700; Email: enge0213@umn.edu

Authors

Zachary Parada − *Department of Biochemistry, Molecular Biology and Biophysics, University of Minnesota, Minneapolis, Minnesota 55455, United States;* orcid.org/0000-0002-7877-3017

Tanner G. Hoog − *Department of Genetics, Cell Biology, and Development, University of Minnesota, Minneapolis, Minnesota 55455, United States;* Present Address: Riptide Therapeutics, Lab 104, 1000 Westgate Drive, St. Paul, Minnesota 55114, United States

Katarzyna P. Adamala − *Department of Biochemistry, Molecular Biology and Biophysics, University of Minnesota, Minneapolis, Minnesota 55455, United States; Department of Genetics, Cell Biology, and Development, University of Minnesota, Minneapolis, Minnesota 55455, United States;* orcid.org/0000-0003-1066-7207

Complete contact information is available at: https://pubs.acs.org/10.1021/acsomega.4c10720

Notes

The authors declare no competing financial interest.

■ ACKNOWLEDGMENTS

We gratefully acknowledge members of the Engelhart and Adamala laboratories for helpful discussions. Research reported in this publication was supported by the National Institute of General Medical Sciences of the National Institutes of Health under award number R01GM152459 (to A.E.E.).

■ REFERENCES

(1) Yang, D. G-Quadruplex DNA and RNA. In *Methods Mol. Biol.*; Methods in molecular biology (Clifton, N.J.); Springer New York: New York, NY, 2019; pp 1−24.

(2) Monsen, R. C.; Trent, J. O.; Chaires, J. B. G-Quadruplex DNA: A Longer Story. *Acc Chem. Res.* **2022**, *55* (22), 3242−3252.

(3) Autour, A.; C Y Jeng, S.; D Cawte, A.; Abdolahzadeh, A.; Galli, A.; Panchapakesan, S. S. S.; Rueda, D.; Ryckelynck, M.; Unrau, P. J. Fluorogenic RNA Mango Aptamers for Imaging Small Non-Coding RNAs in Mammalian Cells. *Nat. Commun.* **2018**, *9* (1), No. 656.

(4) You, M.; Litke, J. L.; Wu, R.; Jaffrey, S. R. Detection of Low-Abundance Metabolites in Live Cells Using an RNA Integrator. *Cell Chem. Biol.* **2019**, *26* (4), 471−481.e3.

(5) Kim, H.; Jaffrey, S. R. A Fluorogenic RNA-Based Sensor Activated by Metabolite-Induced RNA Dimerization. *Cell Chem. Biol.* **2019**, *26* (12), 1725−1731.e6.

(6) Yang, H.; Zhou, Y.; Liu, J. G-Quadruplex DNA for Construction of Biosensors. *Trends Analyt. Chem.* **2020**, *132*, No. 116060.
(7) Alberti, P.; Mergny, J.-L. DNA Duplex-Quadruplex Exchange as the Basis for a Nanomolecular Machine. *Proc. Natl. Acad. Sci. U.S.A.* **2003**, *100* (4), 1569−1573.
(8) Alberti, P.; Bourdoncle, A.; Sacc, B.; Lacroix, L.; Mergny, J.-L. DNA Nanomachines and Nanostructures Involving Quadruplexes. *Org. Biomol. Chem.* **2006**, *4* (18), 3383.
(9) Sen, D.; Poon, L. C. H. RNA and DNA Complexes with Hemin [Fe(III) Heme] Are Efficient Peroxidases and Peroxygenases: How Do They Do It and What Does It Mean? *Crit. Rev. Biochem. Mol. Biol.* **2011**, *46* (6), 478−492.
(10) Ibrahim, H.; Mulyk, P.; Sen, D. DNA G-Quadruplexes Activate Heme for Robust Catalysis of Carbene Transfer Reactions. *ACS Omega* **2019**, *4* (12), 15280−15288.
(11) Hoog, T. G.; Pawlak, M. R.; Aufdembrink, L. M.; Bachan, B. R.; Galles, M. B.; Bense, N. B.; Adamala, K. P.; Engelhart, A. E. Switchable DNA-Based Peroxidases Controlled by a Chaotropic Ion. *Chembiochem* **2022**, *23*, No. e202200090.
(12) Hoog, T. G.; Pawlak, M. R.; Bachan, B. F.; Engelhart, A. E. DNA G-Quadruplexes Are Uniquely Stable in the Presence of Denaturants and Monovalent Cations. *Biochem. Biophys. Rep.* **2022**, *30*, No. 101238.
(13) Adrian, M.; Heddi, B.; Phan, A. T. NMR Spectroscopy of G-Quadruplexes. *Methods* **2012**, *57* (1), 11−24.
(14) Campbell, N.; Collie, G. W.; Neidle, S. Crystallography of DNA and RNA G-quadruplex Nucleic Acids and Their Ligand Complexes. *Curr. Protoc. Nucleic Acid Chem.* **2012**, *50* (1), 17−26, DOI: 10.1002/0471142700.nc1706s50.
(15) Warner, K. D.; Chen, M. C.; Song, W.; Strack, R. L.; Thorn, A.; Jaffrey, S. R.; Ferré-D'Amaré, A. R. Structural Basis for Activity of Highly Efficient RNA Mimics of Green Fluorescent Protein. *Nat. Struct. Mol. Biol.* **2014**, *21* (8), 658−663.
(16) Huang, H.; Suslov, N. B.; Li, N.-S.; Shelke, S. A.; Evans, M. E.; Koldobskaya, Y.; Rice, P. A.; Piccirilli, J. A. A G-Quadruplex-Containing RNA Activates Fluorescence in a GFP-like Fluorophore. *Nat. Chem. Biol.* **2014**, *10* (8), 686−691.
(17) Allain, C.; Monchaud, D.; Teulade-Fichou, M.-P. FRET Templated by G-Quadruplex DNA: A Specific Ternary Interaction Using an Original Pair of Donor/Acceptor Partners. *J. Am. Chem. Soc.* **2006**, *128* (36), 11890−11893.
(18) del Villar-Guerra, R.; Trent, J. O.; Chaires, J. B. G-quadruplex Secondary Structure Obtained from Circular Dichroism Spectroscopy. *Angew. Chem., Int. Ed.* **2018**, *57* (24), 7171−7175.
(19) Helms, V. Fluorescence Resonance Energy Transfer *Principles of Computational Cell Biology* 2008.
(20) Venkatesan, N.; Seo, Y. J.; Kim, B. H. Quencher-Free Molecular Beacons: A New Strategy in Fluorescence Based Nucleic Acid Analysis. *Chem. Soc. Rev.* **2008**, *37* (4), 648−663.
(21) Kim, K. T.; Veedu, R. N.; Seo, Y. J.; Kim, B. H. Quencher-Free Molecular Beacons as Probes for Oligonucleotides Containing CAG Repeat Sequences. *Chem. Commun.* **2014**, *50* (13), 1561−1563.
(22) Lee, S.; Kim, B. H. Molecular Beacons with and without Quenchers. In *Handbook of Chemical Biology of Nucleic Acids*; Springer Nature Singapore: Singapore, 2022; pp 1−35.
(23) Moreira, B. G.; You, Y.; Behlke, M. A.; Owczarzy, R. Effects of Fluorescent Dyes, Quenchers, and Dangling Ends on DNA Duplex Stability. *Biochem. Biophys. Res. Commun.* **2005**, *327* (2), 473−484.
(24) Phan, A. T. Human Telomeric G-quadruplex: Structures of DNA and RNA Sequences. *FEBS J.* **2010**, *277* (5), 1107−1117.
(25) Engelhart, A. E. RNA Imaging: A Tale of Two G-Quadruplexes. *Nat. Chem. Biol.* **2017**, *13* (11), 1140−1141.
(26) Macaya, R. F.; Schultze, P.; Smith, F. W.; Roe, J. A.; Feigon, J. Thrombin-Binding DNA Aptamer Forms a Unimolecular Quadruplex Structure in Solution. *Proc. Natl. Acad. Sci. U.S.A.* **1993**, *90* (8), 3745−3749.
(27) Jovanovic, S. V.; Simic, M. G. One-Electron Redox Potentials of Purines and Pyrimidines. *J. Phys. Chem. A* **1986**, *90* (5), 974−978.
(28) Seidel, C. A. M.; Schulz, A.; Sauer, M. H. M. Nucleobase-Specific Quenching of Fluorescent Dyes. 1. Nucleobase One-Electron Redox Potentials and Their Correlation with Static and Dynamic Quenching Efficiencies. *J. Phys. Chem. A* **1996**, *100* (13), 5541−5553.
(29) Walter, N. G.; Burke, J. M. Real-Time Monitoring of Hairpin Ribozyme Kinetics through Base-Specific Quenching of Fluorescein-Labeled Substrates. *RNA* **1997**, *3* (4), 392−404.
(30) Draganescu, A.; Hodawadekar, S. C.; Gee, K. R.; Brenner, C. Fhit-Nucleotide Specificity Probed with Novel Fluorescent and Fluorogenic Substrates. *J. Biol. Chem.* **2000**, *275* (7), 4555−4560.
(31) Kurata, S. Fluorescent Quenching-Based Quantitative Detection of Specific DNA/RNA Using a BODIPY(R) FL-Labeled Probe or Primer. *Nucleic Acids Res.* **2001**, *29* (6), 34e−334.
(32) Torimura, M.; Kurata, S.; Yamada, K.; Yokomaku, T.; Kamagata, Y.; Kanagawa, T.; Kurane, R. Fluorescence-Quenching Phenomenon by Photoinduced Electron Transfer between a Fluorescent Dye and a Nucleotide Base. *Anal. Sci.* **2001**, *17* (1), 155−160.
(33) Noble, J. E.; Wang, L.; Cole, K. D.; Gaigalas, A. K. The Effect of Overhanging Nucleotides on Fluorescence Properties of Hybridising Oligonucleotides Labelled with Alexa-488 and FAM Fluorophores. *Biophys. Chem.* **2005**, *113* (3), 255−263.
(34) Maruyama, T.; Shinohara, T.; Hosogi, T.; Ichinose, H.; Kamiya, N.; Goto, M. Masking Oligonucleotides Improve Sensitivity of Mutation Detection Based on Guanine Quenching. *Anal. Biochem.* **2006**, *354* (1), 8−14.
(35) Anisenko, A.; Agapkina, J.; Zatsepin, T.; Yanvarev, D.; Gottikh, M. A New Fluorometric Assay for the Study of DNA-Binding and 3′-Processing Activities of Retroviral Integrases and Its Use for Screening of HIV-1 Integrase Inhibitors. *Biochimie* **2012**, *94* (11), 2382−2390.
(36) Mergny, J. L.; Maurizot, J. C. Fluorescence Resonance Energy Transfer as a Probe for G-Quartet Formation by a Telomeric Repeat. *Chembiochem* **2001**, *2* (2), 124−132.
(37) Mergny, J. L.; Boutorine, A. S.; Garestier, T.; Belloc, F.; Rougée, M.; Bulychev, N. V.; Koshkin, A. A.; Bourson, J.; Lebedev, A. V.; Valeur, B.; et al. Fluorescence Energy Transfer as a Probe for Nucleic Acid Structures and Sequences. *Nucleic Acids Res.* **1994**, *22* (6), 920−928.
(38) Kanvah, S.; Joseph, J.; Schuster, G. B.; Barnett, R. N.; Cleveland, C. L.; Landman, U. Oxidation of DNA: Damage to Nucleobases. *Acc Chem. Res.* **2010**, *43* (2), 280−287.

https://doi.org/10.1021/acsomega.4c10720
ACS Omega 2025, 10, 3176−3181